



Identifying SARS-CoV-2 Variants of Concern through Saliva-Based RT-qPCR by Targeting Recurrent Mutation Sites

 Rachel E. Ham,^a Austin R. Smothers,^{a,b} Rui Che,^{a,c} Keegan J. Sell,^a  Congyue Annie Peng,^a  Delphine Dean^{a,b}

^aCenter for Innovative Medical Devices and Sensors (REDDI Lab), Clemson University, Clemson, South Carolina, USA

^bDepartment of Bioengineering, Clemson University, Clemson, South Carolina, USA

^cDepartment of Genetics and Biochemistry, Clemson University, Clemson, South Carolina, USA

Rachel E. Ham and Austin R. Smothers contributed equally to this article. Author order was determined by the corresponding authors after negotiation.

ABSTRACT SARS-CoV-2 variants of concern (VOCs) continue to pose a public health threat which necessitates a real-time monitoring strategy to complement whole genome sequencing. Thus, we investigated the efficacy of competitive probe RT-qPCR assays for six mutation sites identified in SARS-CoV-2 VOCs and, after validating the assays with synthetic RNA, performed these assays on positive saliva samples. When compared with whole genome sequence results, the S Δ 69-70 and ORF1a Δ 3675-3677 assays demonstrated 93.60 and 68.00% accuracy, respectively. The SNP assays (K417T, E484K, E484Q, L452R) demonstrated 99.20, 96.40, 99.60, and 96.80% accuracies, respectively. Lastly, we screened 345 positive saliva samples from 7 to 22 December 2021 using Omicron-specific mutation assays and were able to quickly identify rapid spread of Omicron in Upstate South Carolina. Our workflow demonstrates a novel approach for low-cost, real-time population screening of VOCs.

IMPORTANCE SARS-CoV-2 variants of concern and their many sublineages can be characterized by mutations present within their genetic sequences. These mutations can provide selective advantages such as increased transmissibility and antibody evasion, which influences public health recommendations such as mask mandates, quarantine requirements, and treatment regimens. Our RT-qPCR workflow allows for strain identification of SARS-CoV-2 positive saliva samples by targeting common mutation sites shared between variants of concern and detecting single nucleotides present at the targeted location. This differential diagnostic system can quickly and effectively identify a wide array of SARS-CoV-2 strains, which can provide more informed public health surveillance strategies in the future.

KEYWORDS COVID-19, RT-qPCR, SARS-CoV-2, variants of concern, clinical methods, diagnostics

SARS-CoV-2 has caused more than 407 million infections and more than 5.7 million deaths globally (1). Under neutral genetic drift conditions, SARS-CoV-2 mutates at an estimated rate of 1×10^{-3} substitution per base per year (2). While most mutations are insignificant, some mutations provide selective advantages, such as increased transmissibility and antibody evasion (3–5). Several emerging strains share common nucleotide substitutions at sites that may confer advantageous phenotypic traits (6) and have been deemed variants of concern (VOCs) by public health authorities (7).

The gold standard for differentiating variants of SARS-CoV-2 is whole genome sequencing, which provides excellent resolution of genetic information (8). However, for timely clinical diagnostic applications, such as real-time population surveillance and treatment recommendations, using whole genome sequencing is less feasible because it is not routinely performed in clinical laboratories (9). Additionally, diagnostic sequencing is limited

Editor Heba H. Mostafa, Johns Hopkins Hospital

Copyright © 2022 Ham et al. This is an open-access article distributed under the terms of the [Creative Commons Attribution 4.0 International license](https://creativecommons.org/licenses/by/4.0/).

Address correspondence to Congyue Annie Peng, congyup@clemson.edu, or Delphine Dean, finou@clemson.edu.

The authors declare no conflict of interest.

[This article was published on 12 May 2022 with errors in Table 1. Table 1 has been updated in the current version, posted on 31 May 2022.]

Received 2 March 2022

Accepted 14 April 2022

Published 12 May 2022

by slow turnaround times and high cost per sample (10). This necessitates a low-cost strategy for population-level surveillance of SARS-CoV-2 variants.

RT-qPCR has been used to detect population-level spread of SARS-CoV-2 VOCs, including Alpha (B.1.1.7), Beta (B.1.351), Gamma (P.1), and Delta (B.1.617.2). Alpha was initially traced through populations via S gene target failure (11). This prompted researchers to design assays that rely on target gene failure for detection of deletions or single nucleotide polymorphisms (SNPs) in VOCs (12, 13). However, RT-qPCR assays featuring competitive probes for both reference and mutation sequences increases specificity, providing a more robust strain-typing panel. Such assays have been used to detect Spike (S) deletion 69–70 along with several SNPs characteristic of Alpha and Gamma (14). Additionally, commercially available Spike SNP assays have been used to detect Alpha, Beta, Gamma, and Delta from specimens originating from hospitalized individuals (15). While these assays have been validated for extracted RNA originating from nasopharyngeal swabs, little work has demonstrated the efficacy of RT-qPCR VOC detection in saliva. Saliva-based RT-qPCR has been established as an accurate diagnostic tool comparable to traditional nasopharyngeal swab tests (16–20). Saliva samples provide many benefits, such as room temperature storage (21), simple self-collection of samples (22), and heat-based RNA extraction (23). Furthermore, these advantages have led to its use for many community surveillance programs aimed at testing non-hospitalized patients (24–28). Thus, saliva-based testing warrants examination as a SARS-CoV-2 VOC detection strategy.

Many VOCs contain advantageous genotypes that have emerged independently, indicating that mutation site assays are an effective strategy to monitor emerging dangerous strains (29). We chose to evaluate assays for biochemically significant mutations that also provide differential strain typing for SARS-CoV-2 VOCs, namely, S Δ 69-70, ORF1a Δ 3675-3677, K417T, E484K, E484Q, and L452R. We designed an in-house assay for S Δ 69-70, which has been associated with enhancement of other Spike receptor binding domain (RBD) mutations to increase infectivity in strains such as B.1.1.7 (30). We also designed an assay for ORF1a Δ 3675-3677; although it has not been experimentally linked to improved viral fitness, it has been used to differentiate between Beta and Gamma VOCs (12). We also evaluated the efficacy of TaqPath assays for K417T, E484K, E484Q, and L452R in saliva. Computational modeling has indicated that RBD residues K417, E484, and L452 are critical for increasing viral binding affinity to host cell receptors (31). K417T and K417N SNPs (32) and many substitutions at E484 (33) also reduce viral susceptibility to neutralizing antibodies. Additionally, L452R increases both structural stability and viral fusogenicity, and decreases cell-mediated immune response (34). Conveniently, the currently circulating Omicron variant (B.1.1.529/BA.1) harbors both L452R and S Δ 69-70, so we used these assays to quickly identify its emergence at Clemson University and the surrounding Upstate South Carolina in December 2021. All assays were validated via comparison against whole genome sequence results.

RESULTS

Analytical sensitivity and efficiency of mutation site-specific RT-qPCR assays.

We evaluated the sensitivity of the mutation site-specific RT-qPCR assays via serial 10-fold dilutions of SARS-CoV-2 synthetic RNA of characteristic strains (B.1, B.1.1.7, B.1.351, P.1, B.1.617.1, B.1.617.2). The dilution range for all assays was 4×10^9 to 4×10^6 genome copies/assay (Table 1). We calculated RT-qPCR efficiency for both mutation and reference probes using the equation: $E = -1 + 10^{(-1/\text{slope})}$. Efficiencies of the mutation probes ranged from 89.52% to 112.04% (Table 1, other data included in Table S1 in the supplemental material). R^2 values for all mutation probes were ≥ 0.9927 . The limit of detection (LoD) for S Δ 69-70 was 40 genome copies/assay. LoDs for ORF1a Δ 3675-3677, K417T, E484K, E484Q, and L452R were 4 genome copies/assay. LoD for the control gene (N gene) was also 4 genome copies/assay (Supplemental File 1), which is comparable to the range of detection for saliva-based clinical assays for SARS-CoV-2 screening (16, 35, 36).

Analytical specificity of deletion assays and comparison with saliva samples.

We assessed analytical specificity by performing S Δ 69-70 and ORF1a Δ 3675-3677 deletion assays on synthetic RNA from six characteristic SARS-CoV-2 strains at 4×10^4 genome copies/assay (Fig. 1). We did not observe cross-reactivity or amplification failure

TABLE 1 Performance of RT-qPCR deletion assays in saliva^a

Genome copies/RT-qPCR assay	Mean Cq values +/- SD					
	SΔ69-70	ORF1aΔ3675-3677	K417T	E484K	E484Q	L452R
4 × 10 ⁶	13.11 ± 0.17	12.68 ± 0.11	19.19 ± 0.06	19.12 ± 0.07	19.43 ± 0.07	19.47 ± 0.11
4 × 10 ⁵	16.33 ± 0.04	16.21 ± 0.09	22.27 ± 0.27	22.10 ± 0.04	22.61 ± 0.02	21.20 ± 0.67
4 × 10 ⁴	19.61 ± 0.10	19.40 ± 0.03	24.84 ± 0.57	25.25 ± 0.04	25.72 ± 0.08	24.71 ± 0.23
4 × 10 ³	23.05 ± 0.04	22.80 ± 0.03	29.20 ± 0.86	28.56 ± 0.09	29.26 ± 0.10	27.60 ± 0.14
4 × 10 ²	26.54 ± 0.11	26.23 ± 0.08	34.00 ± 1.07	32.23 ± 0.07	32.99 ± 0.10	31.16 ± 0.10
4 × 10 ¹	30.05 ± 0.15	29.32 ± 0.14	37.14 ± 1.58	35.24 ± 0.26	36.21 ± 0.11	34.48 ± 0.08
4 × 10 ⁰	nd	32.35 ± 0.44	39.85 ± 0.83	38.56 ± 0.33	38.64 ± 0.15	37.06 ± 0.42
E	97.12%	101.44%	89.52%	102.19%	101.40%	112.04%
R ²	0.9997	0.9995	0.9927	0.9994	0.9979	0.9953

^aLimits of detection are in bold.

for any synthetic RNA on either assay. However, the deletion probe from ORF1aΔ3675-3677 produced low fluorescent output. We observed a wide range of fluorescent output from sequenced positive saliva samples ($n = 125$) on both deletion assays. For both deletion assays, samples with low viral copy number (determined by N1 Ct values) were more likely to produce results that could not be resolved. This was especially observed in samples with N1 Ct > 25; 9.09% of samples above this threshold failed on SΔ69-70, while 27.27% of samples above this threshold failed on ORF1aΔ3675-3677 (Supplemental File 2).

Analytical specificity of Spike SNP assays and comparison with saliva samples. We assessed analytical specificity by performing K417T, E484K, E484Q, and L452R assays on synthetic RNA from six characteristic SARS-CoV-2 strains at 4×10^4 genome copies/assay (Fig. 2). We did not observe cross-reactivity for any synthetic RNA on any assay. Amplification failure was expected and occurred for strains lacking both reference and mutation sequences at the locus (e.g., B.1.351 lacks both alleles at K417T, B.1.351 and P.1 lack both alleles at E484Q, and B.1.617.1 lacks both alleles at E484K), which indicates high specificity of all assays per-

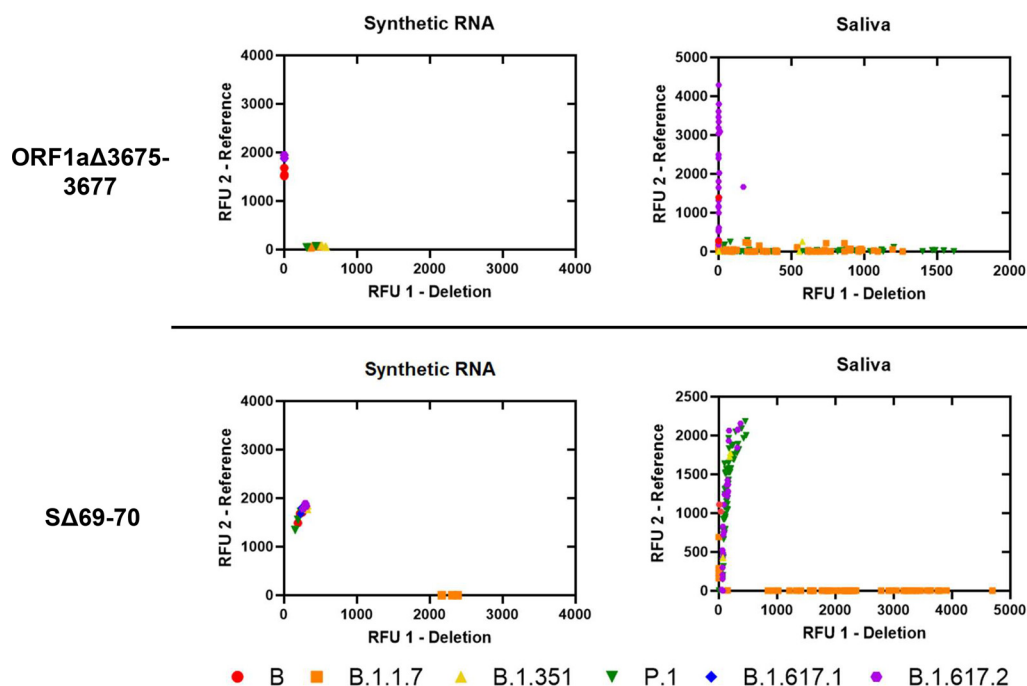


FIG 1 Allelic discrimination plots of deletion assays ORF1aΔ3675-3677 and SΔ69-70. Synthetic RNA controls from six SARS-CoV-2 type strains were amplified in triplicate at 4×10^4 genome copies/assay via TaqPath RT-qPCR along with no template controls. The deletion probe from the ORF1aΔ3675-3677 assay produced low intensity fluorescence. Sequenced positive saliva samples ($n = 125$) were loaded in duplicate to determine the detection range of the assay in saliva. Data were plotted by using the absolute fluorescence of each reporter dye probe.

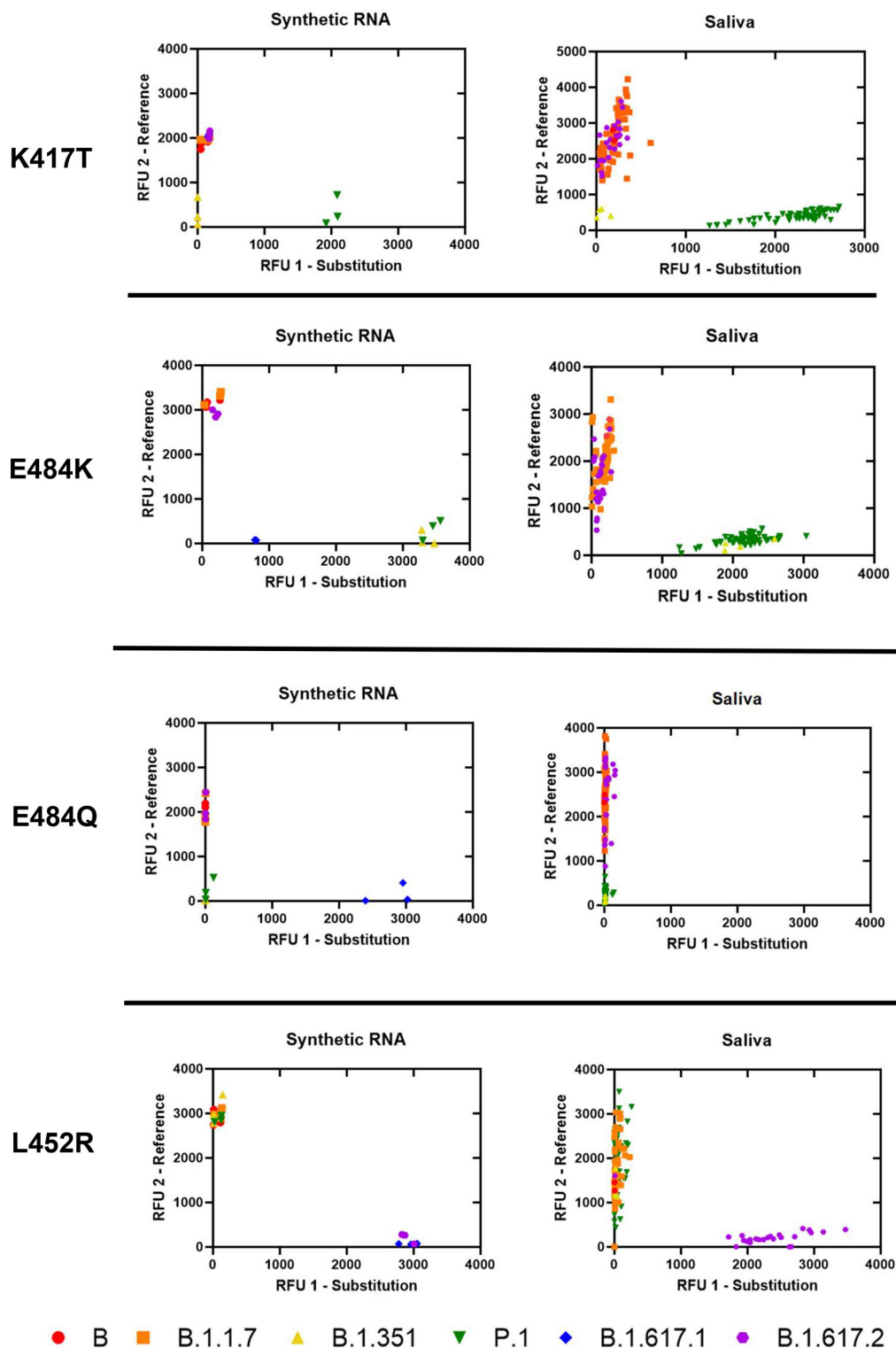


FIG 2 Allelic discrimination plots of SNP assays for Spike K417T, E484K, E484Q, and L452R. Synthetic RNA controls from six SARS-CoV-2 type strains were amplified in triplicate at 4×10^4 genome copies/assay via TaqPath RT-qPCR along with no template controls. Synthetic RNA strains that failed to amplify on K417T, E484K, E484Q, or L452R assays lacked both targeted alleles. Sequenced positive saliva samples ($n = 125$) were loaded in duplicate to determine the detection range of the assay in saliva. Data were plotted by using the absolute fluorescence of each reporter dye probe.

TABLE 2 Performance of deletion assays in saliva^a

Assay	Screening assay result	Whole genome sequencing result		Assay clinical analysis				
		Reference	Deletion	% Accuracy	% Clinical sensitivity	% Clinical specificity	% PPV	% NPV
SΔ69-70	Reference	179	0	93.60	100.0	98.35	94.83	100.0
	Deletion	3	55	[90.57, 96.63]	[100.0]	[96.48, 100.0]	[89.13, 100.0]	[100.0]
	Inconclusive	11	2					
ORF1aΔ3675-3677	Reference	104	0	68.00	100.0	97.20	95.65	100.0
	Deletion	3	66	[62.22, 73.78]	[100.0]	[94.03, 100.0]	[90.84, 100.0]	[100.0]
	Inconclusive	14	63					

^aUpper-bound values cannot exceed 100.0%. This applies to all measurements. 95% confidence interval is represented in brackets.

formed on synthetic RNA. In saliva, we observed tight clustering of fluorescent output from sequenced positive samples ($n = 125$) on all SNP assays. Furthermore, of the 96 replicates that produced an inconclusive result on individual SNP assays, 74 were due to the presence of an alternate allele: 70 replicates containing E484K (B.1.351 and P.1 lineages) were inconclusive on E484Q, 4 replicates containing K417N were inconclusive for K417T (B.1.351 lineage and AY.2 sublineage) (Supplemental File 3 in the supplemental material). All 96 replicates still produced a presumptive strain identification based on the results for the other five assays.

Clinical performance of deletion assays and spike SNP assays in saliva. We compared assay results with whole genome sequence results to determine clinical sensitivity and specificity (Tables 2 and 3). True negatives and true positives are defined as correctly called reference and mutation sequences, respectively. False negatives are defined as incorrectly called reference sequences when the mutation sequence is present, and false positives are defined as incorrectly called mutation sequences when the reference sequence is present. Samples that produced N1 Ct values beyond the limit of detection were considered invalid. For each assay, sample results with allele-specific Ct values above the assay limit of detection were considered inconclusive. Furthermore, due to possible nonspecific binding in the SNP assays, sample results with relative fluorescent output (RFU) values outside of the 99% confidence interval (95% for L452R) of allele-specific RFU were also considered inconclusive (Supplemental Files 4 and 5, logic shown in Fig. S3 in the supplemental material).

We calculated the total accuracies, individual probe accuracies, clinical sensitivity and specificity, as well as positive and negative predictive values: (%PPV and %NPV, respectively) for the deletion assays (Table 2). The total accuracy of SΔ69-70 was 93.6% (95% CI: [90.57, 96.63]);

TABLE 3 Performance of Spike SNP assays in saliva^a

Assay	Screening assay result	Whole genome sequencing result			Assay clinical analysis				
		Reference	Substitution	Alternate	% Accuracy	% Clinical sensitivity	% Clinical specificity	% PPV	% NPV
K417T	Reference	176	0	0	99.20	97.30	100.0	100.0	98.88
	Substitution	0	64	0	[98.10, 100.0 ^a]	[93.55, 100.0]	[100.0]	[100.0]	[97.33, 100.0]
	Inconclusive	2	0	8					
E484K	Reference	173	0	0	96.40	88.31	100.0	100.0	95.05
	Substitution	0	68	0	[94.09, 98.71]	[80.67, 95.95]	[100.0]	[100.0]	[91.90, 98.20]
	Inconclusive	2	7	0					
E484Q	Reference	179	0	0	99.60	98.59	100.0	100.0	99.44
	Substitution	0	0	0	[98.88, 100.0]	[95.83, 100.0]	[100.0]	[100.0]	[98.35, 100.0]
	Inconclusive	1	0	70					
L452R	Reference	181	2	0	96.80	88.41	100.0	100.0	95.77
	Substitution	0	61	0	[94.62, 98.98]	[80.38, 96.47]	[100.0]	[100.0]	[92.90, 98.64]
	Inconclusive	4	2	0					

^aUpper-bound value cannot exceed 100.0%. This applies to all measurements. 95% confidence interval is represented in brackets.

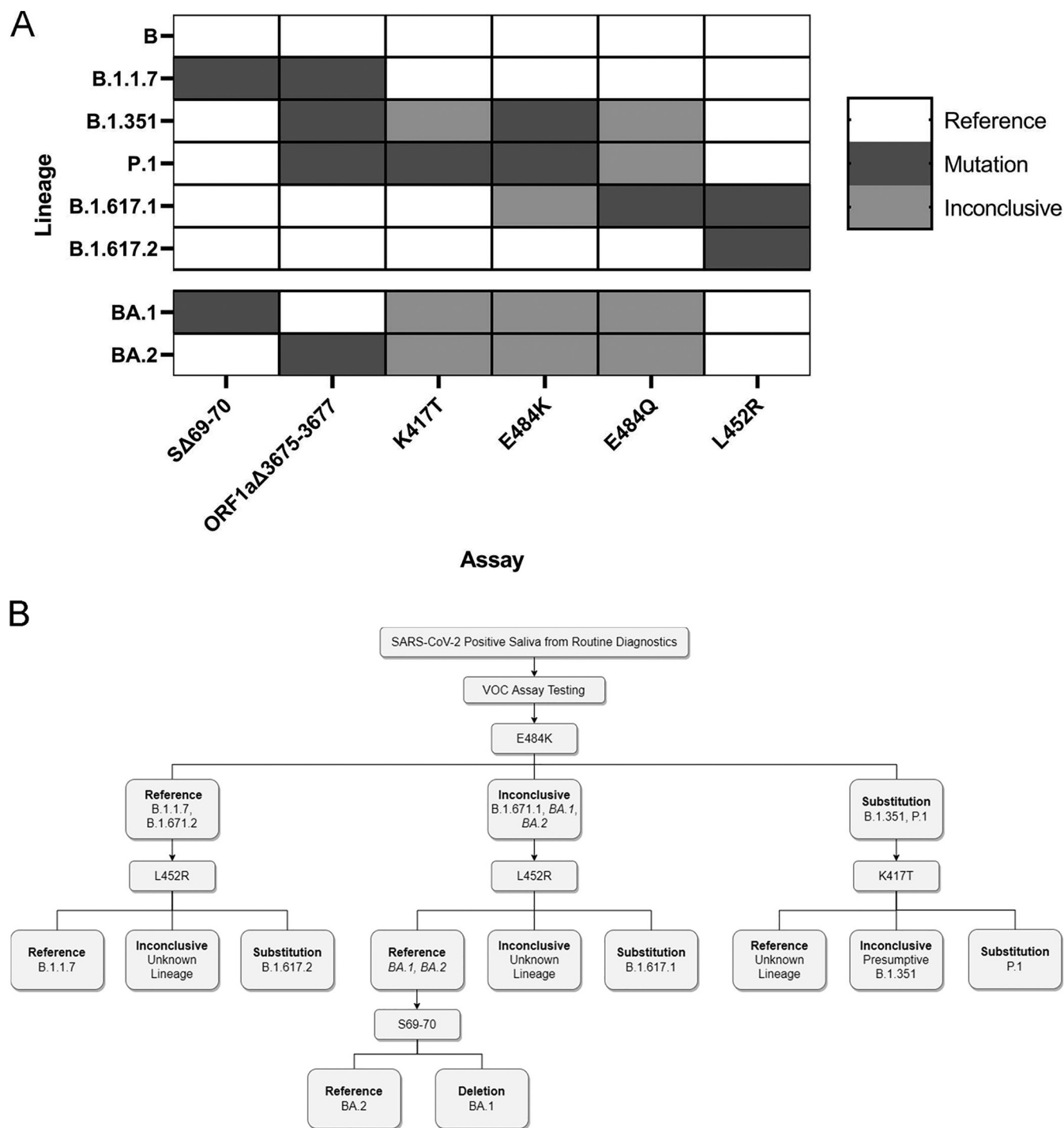


FIG 3 Application and interpretation of differential VOC assays. (A) VOC strain typing by mutation site. Each strain will produce a different combination of results from the six assays. Strains with an alternate allele at the mutation site will produce inconclusive results. BA.1 and BA.2 patterns were determined by publicly available strain data. All other strain results were validated with synthetic RNA. (B) Example of strain-typing workflow using minimal steps. Saliva samples that are determined positive by routine diagnostic testing can be analyzed with various assays that produce differential results for each VOC.

92.68% of reference sequences and 96.49% of deletion sequences could be identified with the associated probes. For ORF1aΔ3675-3677, the total accuracy was 68% (95% CI: [62.22, 73.78]); 85.95% of reference sequences and 51.16% of deletion sequences could be identified with the associated probes. Clinical specificity was 94.82% (95% CI: [96.48, 100.0]) and 95.65% (95% CI: [94.03, 100.0]) for SΔ69-70 and ORF1aΔ3675-3677, respectively. Clinical sensitivity for both deletion assays was 100.0%. The N gene Ct values from the deletion assays indicated

comparable viral loads even after the samples were stored at -80°C for over 6 months (Supplemental File 2). We also calculated the total accuracies, clinical sensitivity and specificity, as well as positive and negative predictive values for the Spike SNP assays in saliva (Table 3).

Presumptive strain identification of positive saliva samples. Combinatorial results of the six mutation sites we investigated can produce signature identification patterns for each SARS-CoV-2 VOC (Fig. 3A). Consequently, we created a clinical workflow for differential strain typing based on these mutation sites (Fig. 3B). Following assay validation, SARS-CoV-2 positive saliva samples were obtained from December 7 to 16, 2021 ($n = 162$). Based on current circulating strains, we performed the L452R assay and identified 13 samples with reference sequence at this site. We performed the $\Delta 69-70$ assay on these 13 samples and identified 11 with the deletion. All 13 samples were sequenced as previously described and confirmed to be B.1.1.529 B.1.1.529/BA.1 (Omicron). We also screened 183 additional samples from December 17 to 22, 2021 to estimate prevalence of Omicron and identified 107 prospective Omicron-positive saliva samples (Supplemental File 6 in the supplemental material).

DISCUSSION

SARS-CoV-2 VOCs continue to pose a significant threat to public health in the United States, especially with the rapid spread of Delta starting in March 2021(31) and, most recently, Omicron in early December 2021 (32). High transmission rates and the related clinical outcomes of these VOCs necessitate affordable and expeditious public health surveillance strategies. The lack of adequate and efficient SARS-CoV-2 variant surveillance has hindered the evaluation of clinical outcomes related to VOCs (34). To address these limitations, our lab implemented a simple VOC screening method following our established saliva-based SARS-CoV-2 testing procedure (35). We perform weekly surveillance testing of the entire population at Clemson University (25) and provide free testing to the surrounding community (24), which allows for real-time monitoring of current and future VOCs.

Deletion and SNP assay analyses. We designed two standard RT-qPCR assays for the SARS-CoV-2 deletion sites $\Delta 69-70$ and ORF1a $\Delta 3675-3677$. The accuracy of the $\Delta 69-70$ assay in saliva was 93.6% (95% CI: [90.57, 96.63]) (Table 2). Two B.1.1.7 samples produced false negative results for both deletion assays, possibly due to nonspecific binding of both reference probes. The accuracy of the ORF1a $\Delta 3675-3677$ assay was 68.0% (95% CI: [62.22, 73.78]); 85.9% of reference sequences could be successfully identified with the reference probe, but only 51.1% of deletion sequences could be successfully identified with the deletion probe. We believe this is due to the relative fluorescence intensity from the competitive probe pair rather than binding affinity or reaction efficiency, as both probes produced replicable amplification from synthetic RNA. The reference probe was tagged with the SUN fluor (37), which produces high fluorescent output that can prevent the thermocycler from identifying amplification from the weaker Cy5-tagged deletion probe. We attempted to account for this by adjusting probe mixing ratios, but this did not improve the fluorescent output of the Cy5 probe. Altering the probe pairing would likely improve the efficacy of this assay. We also performed both assays using the Luna One-Step RT-qPCR System (New England Biolabs, Ipswich, MA) but were unable to detect signal from the SUN probe for ORF1a $\Delta 3675-3677$ reference sequence.

We validated four TaqPath Spike SNP assays in saliva for SARS-CoV-2 substitution sites. The accuracies of K417T, E484K, E484Q, and L452R assays were $\geq 96.4\%$ (Table 3). Even in low viral load samples, saliva does not confound the fidelity of the assays, as the targeted sequences were accurately identified. Moreover, none of the competitive probes produced amplification at sites with an alternate allele. We did observe low-level amplification from off-target binding in the E484K, K417T, and L452R assays. High concentrations of minor groove binding probes can produce background fluorescent signal (38). We could not further investigate if the probe concentration ratio was causing background signal because the commercial kits were pre-mixed. However, because the assays produced well-separated signal clusters, a genotype could still be determined for samples with low-level off-target amplification.

Probe detection parameters and analysis. We determined the Ct cutoff value for each deletion and SNP assay using the absolute quantification approach estimated from analytical sensitivity (39) and observed inconsistencies in the deletion assay limits of

detection. In the S Δ 69-70 assay, the internal control probe passed the Ct threshold earlier than the deletion probe across the 10-fold dilution series except for the lowest dilution, which showed a reversed relationship (4×10 genome copies) (Supplemental File 1 in the supplemental material). Therefore, we opted to use the lower deletion probe Ct cutoff for the S Δ 69-70 assay in saliva. Additionally, both assays were more likely to produce inconclusive results in saliva as the viral load decreased (indicated by N1 Ct value); this effect was more evident in the ORF1a Δ 3675-3677 assay (Supplemental File 2).

Limits of detection inconsistencies were not observed with the SNP assays. However, nonspecific binding of the reference probes necessitated additional RFU cutoff parameters (Fig. S3 in the supplemental material). For both deletion and SNP assays, we included both a reference and mutation control to provide a suitable constant for absolute quantification of Ct values to account for technical limitations (40). This allowed for objective regulation of the RFU cutoff parameters to minimize investigator bias.

Public health surveillance applications. We developed an efficient strain-typing strategy to minimize the number of reactions necessary to differentiate between all common VOCs that had been characterized up to 22 December 2021 (Fig. 3). This workflow is flexible based on publicly available data regarding local strain composition. We demonstrated this by monitoring SARS-CoV-2 positive samples to detect the Omicron variant from 7 to 22 December 2021 by prioritizing distinct mutation sites between Delta and Omicron (specifically, L452R and S Δ 69-70). We screened 345 positive samples, and we expedited 13 suspect samples for whole genome sequencing when the results did not match the established pattern for Delta. This allowed us to confirm the presence of Omicron within days of sample collection.

RT-qPCR screening for VOCs provided a strain composition estimate in December 2021 that allowed our public health surveillance team to adjust SARS-CoV-2 testing and health recommendations in a time-sensitive manner. This would not have been possible solely relying on whole genome sequencing because of slow turnaround time and cost. Furthermore, our assay set was capable of distinguishing AY.2, a subvariant of Delta, from other lineages in the Delta clade. Taken together, these results demonstrate that our assay set is robust and monitors an adequate number of sites to identify emerging strains. Finally, presumptive strain identification also influenced patient treatment recommendations from our collaborating physicians. Specifically, physicians recommended sotrovimab (41) for COVID-19 treatment, as Delta was the predominant circulating strain at the time. Our assays indicated patient samples were positive for Omicron, which is resistant to monoclonal antibody treatment (42). This allowed for physicians to pursue other treatment avenues.

Although our assay workflow is robust and can identify many emerging strains, increasing the number of targeted mutation sites further enhances the potential for strain differentiation. Any number of assays can be used in combination to expand the workflow, and assay order can be prioritized based on high-prevalence strains, however, it is important to prioritize recurring mutation sites (e.g., E484) in SARS-CoV-2 VOCs (43) to maintain time- and cost-effectiveness. To address this, we are validating Spike SNP assays for K417N, N501Y, and G339D as these mutations have emerged independently in multiple lineages.

Expanding the assay set is also advantageous for detecting strains that contain many alternate alleles at targeted mutation sites, such as BA.1 and BA.2 (Fig. 3A). If an alternate allele is present at the target site, the specificity of minor groove binding prevents either reference or mutation probe from binding to the sequence. Therefore, amplification does not occur for these reactions and provides no affirmative results. We recommend assay combinations that minimize the number of undetermined results since these are indistinguishable from assay failures without whole genome sequencing. For instance, it is better to use the E484Q assay rather than the E484K assay to differentiate between the Kappa and Delta variants because one of the probes will produce amplification if there is adequate viral content. Our data show that low viral load samples have an increased likelihood to produce inconclusive results (Supplemental File 2). Therefore, we recommend running samples that produce many undetermined results on an assay that targets the N gene (e.g., S Δ 69-70 or ORF1a Δ 3675-3677) or

TABLE 4 RT-qPCR assays for deletion and substitution sites in SARS-CoV-2 variants of concern

Assay	Manufacturer	Names and 5' → 3' Sequences	Fluorophore
SΔ69-70	IDT	SΔ69-70 Fw primer; TCAACTCAGGACTTGTCTTACCT Rv primer; TGGTAGGACAGGGTTATCAAAC Ref probe; Cy5668/CCATGCTAT/TAO/ACATGTCTCTGGGAC/IBRQ Del probe; HEX/CCATGCTAT/ZEN/CTCTGGGACCAATG/IABkFQ	^a - Cy5 HEX
†ORF1aΔ3675-3677	IDT	ORF1aΔ3675-3677 Fw primer; TGCCTGCTAGTTGGGTGATG Rv primer; TGCTGTCATAAGGATTAGTAACACT Ref probe; SUN/CTAGTTTGT/ZEN/CTGGTTTTAAGCTAA/IABkFQ Del probe; Cy5668/GGTTGATAC/TAO/TAGTTTGAAGCTAA/IABRQ	- - Cy5 SUN
K417N, E484K, L452R, E484Q	ThermoFisher TaqMan	Reference probe ^b Substitution probe ^b	FAM VIC

^a-, indicates that there is no fluorophore for those entries.

^bSequences are unavailable from the manufacturer.

any alternative assay (16, 35, 36) to verify adequate viral load (Ct < assay limit of detection). This eliminates the possibility of undetermined results related to poor quality samples.

Depending on cost analysis, we would also like to implement multiplexed SNP assays. Currently, none of the assays can be multiplexed as they contain overlapping fluorophores. However, custom minor groove binding probe sets can be modified with up to four unique fluorophores that could provide results for two SNPs in the same reaction. Custom probes are more expensive but can reduce the complexity of the workflow. New predictive computational tools can identify recurring mutation sites correlated to emerging strains (44, 45), which can expedite RT-qPCR test development for real-time monitoring. Following presumptive identification, whole genome sequencing of select samples should still be performed to ensure the most accurate surveillance strategy.

MATERIALS AND METHODS

RT-qPCR primer and probe design for deletion assays SΔ69-70 and ORF1aΔ3675-3677. Consensus genome sequences from Alpha (EPI_ISL_710528), Beta (EPI_ISL_678597), Gamma (EPI_ISL_792683), Delta (EPI_ISL_1544014), and a reference strain (MN908947.3) were downloaded from GenBank. Sequences were aligned using ClustalW (SnapGene v.5.4.2) to confirm that the deletions were only present in VOCs. Validated primer sets designed for the N gene (36), SΔ69-70 (12), and ORF1aΔ3675-3677 regions (12) matched this alignment. Each assay includes three probes tagged with different fluorophores: one targeting the N gene, one targeting the reference sequence, and one targeting the deletion sequence (Table 4). Novel reference and deletion probes were designed with short sequences to prevent primer dimer formation in a multiplex assay format. All probes were double quenched to minimize noise and maximize endpoint fluorescence.

Optimization of deletion and SNP assays. SΔ69-70 and ORF1aΔ3675-3677 deletion assays were performed with TaqPath 1-Step RT-qPCR kit (Thermo Fisher, Waltham MA, USA) using reactions with 4 μL of template in a final volume of 20 μL. Primers and probes were used at final concentrations of 500 nM for each primer and 125 nM for each probe (Integrated DNA Technologies, Coralville, IA). SARS-CoV-2 TaqMan Assays for S substitutions K417T, E484K, E484Q, and L452R were performed per manufacturer's instructions (Thermo Fisher) with 4 μL of template. Thermocycler conditions are described in Table S2 in the supplemental material.

Standard curve and limit of detection analysis. We used TWIST synthetic SARS-CoV-2 RNA control 2 (GenBank ID: MN908947.3), control 14 (GISAID ID: EPI_ISL_710528), control 16 (GISAID ID: EPI_ISL_678597), control 17 (GISAID ID: EPI_ISL_792683), control 18 (GISAID ID: EPI_ISL_1662307), and control 23 (GISAID ID: EPI_ISL_1544014) (Twist Biosciences, San Francisco, CA) to determine the limits of detection of the screening RT-qPCR assays. We tested a seven-fold dilution series from 1,000,000 copies/μL to 1 copy/μL for both reference and mutation RNA controls in triplicate for each assay and confirmed that the lowest concentration was detected in all three replicates. Standard curves were created to find correlation coefficients and determine efficiencies of each probe and primer set.

Specificity analysis. We performed all six assays on TWIST synthetic SARS-CoV-2 RNA control 2 (B), control 14 (B.1.1.7), control 16 (B.1.351), control 17 (P.1), control 18 (B.1.617.1), and control 23 (B.1.617.2) (Twist Biosciences, San Francisco, CA). All synthetic RNA was diluted to 10,000 copies/μL and each reaction was performed in triplicate. Allelic discrimination plots were created for each assay to determine cross-reactivity of reference and mutation probes at each target site.

Whole genome sequencing. Ethical review for this study was obtained by the Institutional Review Board of Clemson University. This study uses archived deidentified samples and data. The samples and data sets

were stripped of patient identifiers prior to any SARS-CoV-2 sequencing and experiments for this study. Heat-treated saliva samples were sequenced at a commercial lab (Premier Medical Laboratory Services, Greenville, SC). RNA was extracted from saliva samples via magnetic beads (Omega Bio-Tek, Norcross, GA) and recovered SARS-CoV-2 RNA quantity was assessed via Logix Smart Assay (Codiagnosics, Salt Lake City, UT). Samples with sufficient RNA quality were processed and sequenced on either an Illumina NovaSeq 6000 or NextSeq500/550 flow cell. Sequences were demultiplexed, assembled, and analyzed with DRAGEN COVID Lineage (Illumina, v.3.5.3).

Saliva screening. We performed all six assays in duplicate on sequenced saliva samples ($n = 125$) that had greater than 95% non-N genome coverage to validate assay parameters. Saliva samples from the university SARS-CoV-2 surveillance program (24, 25) were heat-treated to extract viral RNA and confirmed to be SARS-CoV-2 positive via RT-qPCR (35). Due to extended storage time at -80°C for some positive samples, sample validity was determined using N1 Ct values to account for possible degradation. Sample identification was performed using a single-blind method and all assays were performed on all samples, removing investigator bias. We selected lineages B.1.1.7 (Alpha, $n = 30$), B.1.351 (Beta, $n = 2$), P.1 (Gamma, $n = 32$), B.1.617.2/AY (Delta, $n = 32$), and other lineages not of concern ($n = 29$). We did not have any confirmed B.1.617.1 (Kappa, $n = 0$) saliva samples. Five samples were excluded from analysis due to inadequate N1 amplification. GenBank accession numbers of all the sequences used to validate the assays in saliva are available in supplemental data in the supplemental material.

Statistical analysis. We calculated accuracies ($[\text{true positives} + \text{true negatives}]/\text{sample size} \times 100\%$), clinical sensitivity ($[\text{true positives}/(\text{true positives} + \text{false negatives})] \times 100\%$), clinical specificity ($[\text{true negatives}/(\text{true negatives} + \text{false positives})] \times 100\%$), positive predictive value (PPV) ($[\text{true positives}/(\text{true positives} + \text{false positives})] \times 100\%$), and negative predictive value (NPV) ($[\text{true negatives}/(\text{true negatives} + \text{false negatives})] \times 100\%$) of the assays using whole genome sequencing results for comparison. We also calculated 95% confidence intervals for all measurements.

Data availability. All the data, worksheets, and standard curves used for this study are available in the Supplemental Files. The listing of available sequences on GenBank and GISAID for each sample are listed in Supplemental File 3, Sequenced Sample List with GenBank and GISAID Information.

SUPPLEMENTAL MATERIAL

Supplemental material is available online only.

SUPPLEMENTAL FILE 1, XLSX file, 0.1 MB.

SUPPLEMENTAL FILE 2, XLS file, 0.5 MB.

SUPPLEMENTAL FILE 3, XLS file, 0.1 MB.

SUPPLEMENTAL FILE 4, XLSX file, 0.2 MB.

SUPPLEMENTAL FILE 5, XLSX file, 0.3 MB.

SUPPLEMENTAL FILE 6, XLSX file, 0.03 MB.

SUPPLEMENTAL FILE 7, PDF file, 0.4 MB.

ACKNOWLEDGMENTS

We thank Clemson University's administration, medical staff, and clinical lab employees at the REDDI Lab who helped implement and manage SARS-CoV-2 testing. Thank you to Kylie King for managing the biorepository of positive saliva samples. Thank you to Mark Blenner for initial project consulting. We thank Jeremiah Carpenter, Kaitlyn Williams, Sujata Srikanth, and Stevin Wilson for sequencing workflow management, as well as Jessie Boulos for performing clinical sample screening. Thank you to Kylie King for technical assistance as well as critical reading of the manuscript. Thank you to Creative Inquiry students for standard curve and analytical specificity data collection. This project was funded by SC Governor and Joint Bond Review Committee, NIH NIGMS 3P20GM121342-03S1, NSF 1757658, and Clemson University Office of Creative Inquiry and Undergraduate Research.

R.E.H., A.R.S., and C.A.P. contributed to the conception of the manuscript. R.E.H., A.R.S., and R.C. designed project methodology. R.E.H., R.C., A.R.S., and K.J.S. performed the experiments. R.H. mentored and instructed Creative Inquiry undergraduate students. R.E.H. and A.R.S. curated, analyzed, and presented data, as well as drafted the manuscript. R.E.H., A.R.S., D.D., and C.A.P. contributed to close analysis and editing of the manuscript. All authors contributed to, read, and approved the submitted manuscript.

REFERENCES

1. Dong E, Du H, Gardner L. 2020. An interactive web-based dashboard to track COVID-19 in real time. *Lancet Infect Dis* 20:533–534. [https://doi.org/10.1016/S1473-3099\(20\)30120-1](https://doi.org/10.1016/S1473-3099(20)30120-1).
2. Duchene S, Featherstone L, Haritopoulou-Sinanidou M, Rambaut A, Lemey P, Baele G. 2020. Temporal signal and the phylodynamic threshold of SARS-CoV-2. *Virus Evol* 6:veaa061. <https://doi.org/10.1093/ve/veaa061>.
3. Harvey WT, Carabelli AM, Jackson B, Gupta RK, Thomson EC, Harrison EM, Ludden C, Reeve R, Rambaut A, Peacock SJ, Robertson DL, COVID-19 Genomics UK (COG-UK) Consortium. 2021. SARS-CoV-2 variants, spike

- mutations and immune escape. *Nat Rev Microbiol* 19:409–424. <https://doi.org/10.1038/s41579-021-00573-0>.
4. Davies NG, Jarvis CI, Covid-19 C, Group W, Edmunds WJ, Jewell NP, Diaz-Ordaz K, Keogh RH, CMMID COVID-19 Working Group. 2021. Increased mortality in community-tested cases of SARS-CoV-2 lineage B.1.1.7. *Nature* 593:270–274. <https://doi.org/10.1038/s41586-021-03426-1>.
 5. Campbell F, Archer B, Laurenson-Schafer H, Jinnai Y, Konings F, Batra N, Pavlin B, Vandemaële K, Van Kerkhove MD, Jombart T, Morgan O, De Waroux OLP. 2021. Increased transmissibility and global spread of SARS-CoV-2 variants of concern as at June 2021. *Eurosurveillance* 26:1–6. <https://doi.org/10.2807/1560-7917.ES.2021.26.24.2100509>.
 6. Oude Munnink BB, Worp N, Nieuwenhuijse DF, Sikkema RS, Haagmans B, Fouchier RAM, Koopmans M. 2021. The next phase of SARS-CoV-2 surveillance: real-time molecular epidemiology. *Nat Med* 27:1518–1524. <https://doi.org/10.1038/s41591-021-01472-w>.
 7. World Health Organization. 2021. Guidance for surveillance of SARS-CoV-2 variants: interim guidance, 9 August 2021. World Health Organization, Geneva.
 8. Armstrong GL, MacCannell DR, Taylor J, Carleton HA, Neuhaus EB, Bradbury RS, Posey JE, Gwinn M. 2019. Pathogen Genomics in Public Health. *N Engl J Med* 381:2569–2580. <https://doi.org/10.1056/NEJMs1813907>.
 9. Crawford DC, Williams SM. 2021. Global variation in sequencing impedes SARS-CoV-2 surveillance. *PLoS Genet* 17:e1009620. <https://doi.org/10.1371/journal.pgen.1009620>.
 10. Rossen JWA, Friedrich AW, Moran-Gilad J, ESCMID Study Group for Genomic and Molecular Diagnostics (ESGMD). 2018. Practical issues in implementing whole-genome-sequencing in routine diagnostic microbiology. *Clin Microbiol Infect* 24:355–360. <https://doi.org/10.1016/j.cmi.2017.11.001>.
 11. Borges V, Sousa C, Menezes L, Gonçalves AM, Picão M, Almeida JP, Vieira M, Santos R, Silva AR, Costa M, Carneiro L, Casaca P, Pinto-Leite P, Peraltasantos A, Isidoro J, Duarte S, Vieira L, Guiomar R, Silva S, Nunes B, Gomes JP. 2021. Tracking SARS-CoV-2 lineage B.1.1.7 dissemination: insights from nationwide spike gene target failure (SGTF) and spike gene late detection (SGTL) data, Portugal, week 49 2020 to week 3 2021. *Eurosurveillance* 26:1–6. <https://doi.org/10.2807/1560-7917.ES.2021.26.10.2100130>.
 12. Vogels CB, Breban MI, Ott IM, Alpert T, Petrone ME, Watkins AE, Kalinich CC, Earnest R, Rothman JE, Goes de Jesus J, Morales Claro I, Magalhães Ferreira G, Crispim MA, Cade Genomic Network B-U, Singh L, Tegally H, Anyaneji UJ, Hodcroft EB, Mason CE, Khullar G, Metti J, Dudley JT, MacKay MJ, Nash M, Wang J, Liu C, Hui P, Murphy S, Neal C, Laszlo E, Landry ML, Muyombwe A, Downing R, Razeq J, de Oliveira T, Faria NR, Sabino EC, Neher RA, Fauver JR, Grubaugh ND, Network for Genomic Surveillance in South Africa. 2021. Multiplex qPCR discriminates variants of concern to enhance global surveillance of SARS-CoV-2 Network for Genomic Surveillance in South Africa. *PLoS Biol* 19:e3001236. <https://doi.org/10.1371/journal.pbio.3001236>.
 13. Babiker A, Immergluck K, Stampfer SD, Rao A, Bassit L, Su M, Nguyen V, Stittleburg V, Ingersoll JM, Bradley HL, Mavigner M, Schoof N, Kraft CS, Chahroudi A, Schinazi RF, Martin GS, Piantadosi A, Lam WA, Waggoner JJ. 2021. Single-amplicon multiplex real-time reverse transcription-PCR with tiled probes to detect SARS-CoV-2 spike mutations associated with variants of concern. *J Clin Microbiol* 59:e0144621. <https://doi.org/10.1128/JCM.01446-21>.
 14. Vega-Magaña N, Sá Nchez-Sá Nchez R, Herná Ndez-Bello J, Antony Venancio-Landeros A, Peña-Rodríguez M, Alejandra Vega-Zepeda R, Galindo-Ornelas B, Díaz-Sá Nchez M, García-Chagollá M, Macedo-Ojeda G, Patricio García-González O, Francisco Muñoz-Valle J, Musso N, Hung CK, Valenzuela-Fernandez A, Nchez-Sá Nchez SR, Ndez-Bello HJ, Nchez D-SM. 2021. RT-qPCR assays for rapid detection of the N501Y, 69–70del, K417N, and E484K SARS-CoV-2 mutations: a screening strategy to identify variants with clinical impact. *Front Cell Infect Microbiol* 11:672562. <https://doi.org/10.3389/fcimb.2021.672562>.
 15. Pham VH, Vo CD, Nguyen HM, Pham BT, Le SH, Trần DK, Nguyen QV, Tran VQ, Pham HT, Pham ST, Nguyen NHD. 2021. Real-time PCR detects 4 rapid transmission variants of SARS-CoV-2. *Int J Antimicrob Agents* 58:2100354. <https://doi.org/10.1016/j.ijantimicag.2021.106421.83>.
 16. Vogels CBF, Watkins AE, Harden CA, Brackney DE, Shafer J, Wang J, Caraballo C, Kalinich CC, Ott IM, Fauver JR, Kudo E, Lu P, Venkataraman A, Tokuyama M, Moore AJ, Muenker MC, Casanovas-Massana A, Fournier J, Bermejo S, Campbell M, Datta R, Nelson A, Dela Cruz CS, Ko AI, Iwasaki A, Krumholz HM, Mathews JD, Hui P, Liu C, Farhadian SF, Sikka R, Wyllie AL, Grubaugh ND, Anastasio K, Askenase MH, Batsu M, Bickerton S, Brower K, Bucklin ML, Cahill S, Cao Y, Courchaine E, Deluigi G, Earnest R, Geng B, Goldman-Israelow B, Handoko R, Khoury-Hanold W, Kim D, Knaggs L, et al. 2021. SalivaDirect: A simplified and flexible platform to enhance SARS-CoV-2 testing capacity. *Med* 2:263–280.e6. <https://doi.org/10.1016/j.medj.2020.12.010>.
 17. Pasomsub E, Watcharananan SP, Boonyawat K, Janchompoo P, Wongtabtim G, Suksuwan W, Sungkanuparph S, Phuphuakrat A. 2021. Saliva sample as a non-invasive specimen for the diagnosis of coronavirus disease 2019: a cross-sectional study. *Clin Microbiol Infect* 27:285.e1–285.e4. <https://doi.org/10.1016/j.cmi.2020.05.001>.
 18. Griesemer SB, Van Slyke G, Ehrbar D, Strle K, Yildirim T, Centurioni DA, Walsh AC, Chang AK, Waxman MJ, St George K. 2021. Evaluation of specimen types and saliva stabilization solutions for SARS-CoV-2 testing. *J Clin Microbiol* 59:e01418. <https://doi.org/10.1128/JCM.01418-20>.
 19. Bastos ML, Perlman-Arrow S, Menzies D, Campbell JR. 2021. The sensitivity and costs of testing for SARS-CoV-2 infection with saliva versus nasopharyngeal swabs a systematic review and meta-analysis. *Ann Intern Med* 174:501–510. <https://doi.org/10.7326/M20-6569>.
 20. To KKW, Tsang OTY, Yip CCY, Chan KH, Wu TC, Chan JMC, Leung WS, Chik TSH, Choi CYC, Kandamby DH, Lung DC, Tam AR, Poon RWS, Fung AYF, Hung IFN, Cheng VCC, Chan JFW, Yuen KY. 2020. Consistent Detection of 2019 novel coronavirus in saliva. *Clin Infect Dis* 71:841–843. <https://doi.org/10.1093/cid/ciaa149>.
 21. Uwamino Y, Nagata M, Aoki W, Fujimori Y, Nakagawa T, Yokota H, Sakai-Tagawa Y, Iwatsuki-Horimoto K, Shiraki T, Uchida S, Uno S, Kabata H, Ikemura S, Kamata H, Ishii M, Fukunaga K, Kawaoka Y, Hasegawa N, Murata M. 2021. Accuracy and stability of saliva as a sample for reverse transcription PCR detection of SARS-CoV-2. *J Clin Pathol* 74:67–68. <https://doi.org/10.1136/jclinpath-2020-206972>.
 22. Wehrhahn MC, Robson J, Brown S, Bursle E, Byrne S, New D, Chong S, Newcombe JP, Siversten T, Hadlow N. 2020. Self-collection: an appropriate alternative during the SARS-CoV-2 pandemic. *J Clin Virol* 128:104417. <https://doi.org/10.1016/j.jcv.2020.104417>.
 23. Barza R, Patel P, Sabatini L, Singh K. 2020. Use of a simplified sample processing step without RNA extraction for direct SARS-CoV-2 RT-PCR detection. *J Clin Virol* 132:104587. <https://doi.org/10.1016/j.jcv.2020.104587>.
 24. Plumb EV, Ham RE, Napolitano JM, King KL, Swann TJ, Kalbaugh C, Rennett L, Dean D. 2022. Implementation of a rural community diagnostic testing strategy for SARS-CoV-2 in upstate South Carolina. *Front Public Heal* 10:858421. <https://doi.org/10.3389/fpubh.2022.858421>.
 25. Rennett L, McMahan C, Kalbaugh CA, Yang Y, Lumsden B, Dean D, Pekarek L, Colenda CC. 2021. Surveillance-based informative testing for detection and containment of SARS-CoV-2 outbreaks on a public university campus: an observational and modelling study. *Lancet Child Adolesc Heal* 4642:1–9.
 26. Ehrenberg AJ, Moehle EA, Brook CE, Doudna Cate AH, Witkowsky LB, Sachdeva R, Hirsh A, Barry K, Hamilton JR, Lin-Shiao E, McDevitt S, Valentin-Alvarado L, Letourneau KN, Hunter L, Keller A, Pestal K, Frankino PA, Murley A, Nandakumar D, Stahl EC, Tsuchida CA, Gildea HK, Murdock AG, Hochstrasser ML, O'Brien E, Ciling A, Tsitsiklis A, Worden K, Dugast-Darzacq C, Hays SG, Barber CC, McGarrigle R, Lam EK, Ensminger DC, Bardet L, Sherry C, Harte A, Nicolette G, Giannikopoulos P, Hockemeyer D, Petersen M, Urnov FD, Ringeisen BR, Boots M, Doudna JA, IGI SARS-CoV-2 Testing Consortium. 2021. Launching a saliva-based SARS-CoV-2 surveillance testing program on a university campus. *PLoS One* 16:e0251296. <https://doi.org/10.1371/journal.pone.0251296>.
 27. Avendano C, Lilienfeld A, Rulli L, Stephens M, Barrios WA, Sarro J, Pfreder ME, Miranda ML. 2022. SARS-CoV-2 variant tracking and mitigation during in-person learning at a midwestern university in the 2020–2021 school year. *JAMA Netw Open* 5:e2146805. <https://doi.org/10.1001/jamanetworkopen.2021.46805>.
 28. Carmagnola D, Pellegrini G, Canciani E, Henin D, Perrotta M, Forlanini F, Barcellini L, Dellavia C. 2021. Saliva molecular testing for SARS-CoV-2 surveillance in two Italian primary schools. *Child (Basel, Switzerland)*.
 29. Peacock TP, Penrice-Randal R, Hiscox JA, Barclay WS. 2021. SARS-CoV-2 one year on: evidence for ongoing viral adaptation. *J Gen Virol* 102:1584.
 30. Meng B, Kemp SA, Papa G, Dattir R, Ferreira IATM, Marelli S, Harvey WT, Lytras S, Mohamed A, Gallo G, Thakur N, Collier DA, Milcochova P, Duncan LM, Carabelli AM, Kenyon JC, Lever AM, De Marco A, Saliba C, Culap K, Cameroni E, Matheson NJ, Piccoli L, Corti D, James LC, Robertson DL, Bailey D, Gupta RK, COVID-19 Genomics UK Consortium. 2021. Recurrent emergence of SARS-CoV-2 spike deletion H69/V70 and its role in the Alpha variant B.1.1.7. *Cell Rep* 35:109292. <https://doi.org/10.1016/j.celrep.2021.109292>.
 31. Sanchez PRS, Charlie-Silva I, Braz HLB, Bittar C, Freitas Calmon M, Rahal P, Cilli EM. 2021. Recent advances in SARS-CoV-2 Spike protein and RBD mutations comparison between new variants Alpha (B.1.1.7, United Kingdom), Beta (B.1.351, South Africa), Gamma (P.1, Brazil) and Delta (B.1.617.2, India). *J Virus Erad* 7:100054. <https://doi.org/10.1016/j.jve.2021.100054>.

32. Wang L, Cheng G. 2022. Sequence analysis of the emerging SARS-CoV-2 variant Omicron in South Africa. *J Med Virol* 94:1728–1733. <https://doi.org/10.1002/jmv.27516>.
33. Liu Z, VanBlargan LA, Bloyet L-M, Rothlauf PW, Chen RE, Stumpf S, Zhao H, Errico JM, Theel ES, Liebeskind MJ, Alford B, Buchser WJ, Ellebedy AH, Fremont DH, Diamond MS, Whelan SPJ. 2021. Identification of SARS-CoV-2 spike mutations that attenuate monoclonal and serum antibody neutralization. *Cell Host Microbe* 29:477–488. <https://doi.org/10.1016/j.chom.2021.01.014>.
34. Motozono C, Toyoda M, Zahradnik J, Saito A, Nasser H, Tan TS, Ngare I, Kimura I, Uriu K, Kosugi Y, Yue Y, Shimizu R, Ito J, Torii S, Yonekawa A, Shimono N, Nagasaki Y, Minami R, Toya T, Sekiya N, Fukuhara T, Matsuura Y, Schreiber G, Ikeda T, Nakagawa S, Ueno T, Sato K, Genotype to Phenotype Japan (G2P-Japan) Consortium. 2021. SARS-CoV-2 spike L452R variant evades cellular immunity and increases infectivity. *Cell Host Microbe* 29:1124–1136. <https://doi.org/10.1016/j.chom.2021.06.006>.
35. Ham RE, Smothers AR, King KL, Napalitano JM, Swann TJ, Pekarek LG, Blenner MA, Dean D. 2022. Efficient SARS-CoV-2 quantitative reverse transcriptase PCR saliva diagnostic strategy utilizing open-source pipetting robots. *J Vis Exp*. <https://doi.org/10.3791/63395>.
36. Centers for Disease Control. 2021. CDC 2019-nCoV RT-PCR diagnostic panel, National Center for Immunization and Respiratory Diseases (NCIRD), Atlanta, USA.
37. Pazdernik N. 2020. SUN fluorophore: a molecular equivalent to VIC. <https://www.idtdna.com/pages/education/decoded/article/sun-fluorophore-a-molecular-equivalent-to-vic>.
38. Long S, Berkemeier B. 2020. Development and optimization of a simian immunodeficiency virus (SIV) droplet digital PCR (ddPCR) assay. *PLoS One* 15:e0240447. <https://doi.org/10.1371/journal.pone.0240447>.
39. Caraguel CGB, Stryhn H, Gagné N, Dohoo IR, Hammell KL. 2011. Selection of a cutoff value for real-time polymerase chain reaction results to fit a diagnostic purpose: Analytical and epidemiologic approaches. *J Vet Diagn Invest* 23:2–15. <https://doi.org/10.1177/104063871102300102>.
40. Wong ML, Medrano JF. 2005. Real-time PCR for mRNA quantitation. *Bio-techniques* 39:75–85. <https://doi.org/10.2144/05391RV01>.
41. GlaxoSmithKline. 2021. Sotrovimab [package insert]. Research Triangle Park, NC.
42. Aggarwal A, Ospina SA, Walker G, Akerman A, Milogiannakis V, Brilot F, Amatayakul-Chantler S, Roth N, Coppola G, Schofield P, Jackson J, Henry JY, Mazigi O, Langley D, Lu Y, Forster C, Mcallery S, Mathivanan V, Fichter C, Hoppe Ac Munier MI Jack H-M, Cromer D, Darley D, Matthews G, Christ D, Khoury D, Davenport M, Rawlinson W, Kelleher AD, Turville S, Turville SG. 2021. SARS-CoV-2 Omicron: evasion of potent humoral responses and resistance to clinical immunotherapeutics relative to viral variants of concern. medRxiv.
43. Hodcroft EB. 2022. CoVariants: SARS-CoV-2 mutations and variants of interest. <https://covariants.org/>.
44. Negi SS, Schein CH, Braun W. 2022. Regional and temporal coordinated mutation patterns in SARS-CoV-2 spike protein revealed by a clustering and network analysis. *Sci Rep* 12:10. <https://doi.org/10.1038/s41598-022-04950-4>.
45. Rodriguez-Rivas J, Croce G, Muscat M, Weigt M. 2022. Epistatic models predict mutable sites in SARS-CoV-2 proteins and epitopes. *Proc Natl Acad Sci U S A* 119:e2113118119. <https://doi.org/10.1073/pnas.2113118119>.